

# WM-MoE: Weather-aware Multi-scale Mixture-of-Experts for Blind Adverse Weather Removal

Yulin Luo, Rui Zhao, Xiaobao Wei, Jinwei Chen, Yujie Lu, Shenghao Xie, Tianyu Wang, Ruiqin Xiong, Ming Lu, Shanghang Zhang

**Abstract**—Adverse weather removal tasks like deraining, desnowing, and dehazing are usually treated as separate tasks. However, in practical autonomous driving scenarios, the type, intensity, and mixing degree of weather are unknown, so handling each task separately cannot deal with the complex practical scenarios. In this paper, we study the blind adverse weather removal problem. Mixture-of-Experts (MoE) is a popular model that adopts a learnable gate to route the input to different expert networks. The principle of MoE involves using adaptive networks to process different types of unknown inputs. Therefore, MoE has great potential for blind adverse weather removal. However, the original MoE module is inadequate for coupled multiple weather types and fails to utilize multi-scale features for better performance. To this end, we propose a method called Weather-aware Multi-scale MoE (WM-MoE) based on Transformer for blind weather removal. WM-MoE includes two key designs: WEather-Aware Router (WEAR) and Multi-Scale Experts (MSE). WEAR assigns experts for each image token based on decoupled content and weather features, which enhances the model’s capability to process multiple adverse weathers. To obtain discriminative weather features from images, we propose Weather Guidance Fine-grained Contrastive Learning (WGF-CL), which utilizes weather cluster information to guide the assignment of positive and negative samples for each image token. Since processing different weather types requires different receptive fields, MSE leverages multi-scale features to enhance the spatial relationship modeling capability, facilitating the high-quality restoration of diverse weather types and intensities. Our method achieves state-of-the-art performance in blind adverse weather removal on two public datasets and our dataset. We also demonstrate the advantage of our method on downstream segmentation tasks.

**Index Terms**—Blind Weather Removal, Vision Transformer, Mixture-of-Experts (MoE), Contrastive Learning, Deep Learning

## I. INTRODUCTION

In autonomous driving scenarios, adverse weather could severely impact the imaging quality of cameras, leading to the degradation of AI performance [1]. Thus, adverse weather removal is a crucial technique for autonomous driving. Most existing methods handle different weather types separately,

such as deraining, desnowing, and dehazing. They can be divided into three categories: task-specific, task-agnostic, and multi-task-in-one methods. The task-specific methods are designed for a specific type of weather, such as deraining [2]–[7], dehazing [8]–[16], and desnowing [17]–[19]. These methods have a weather-related inductive bias, making them difficult to perform well on other tasks. Task-agnostic methods have a unified solution to different tasks but need to be trained separately [20]–[22], and need users to select specific parameters according to the weather type. The applications of task-agnostic methods are quite limited. Hence, their usefulness is limited as well. Multi-task-in-one methods can handle different types of weather using a single set of parameters [23]–[26], but they still have several limitations. For example, the schemes of defining weather types in existing methods are complex, and mixed weather types are not considered. BIDeN [27] formulates the real-world mixture weather removal as a blind image decomposition task. During training, the multi-domain GAN-based model requires each weather component, which is not available in real scenarios, thus limiting its applicability.

Since the type, intensity, and mixing degree of the weather are unknown in the real world, recent blind weather removal aims to restore corrupted images with unknown weather types. It has gained increasing attention from the community [24], [25], [27], [28]. The key to blind weather removal is dynamically processing the input based on the weather type. Mixture-of-Experts (MoE) [29] is a model that adopts adaptive expert networks to process different inputs with the help of a router. Therefore, MoE has great potential for blind weather removal. Some methods have tried to apply MoE to the weather removal task. HCT-FFN [30] utilizes degradation-aware MoE (DaMoE) to extract local features for restoring spatially-varying rain degradation, DRSformer [31] learns enriched sparse content features for deraining via a mixture of experts feature compensator. DAN-Net [32] employs adaptive gated neural to modulate the outputs of task-specific experts, which can be utilized to deal with the mix of snow and haze. However, they neglect using weather features to guide expert selection for the blind weather removal task.

Our work also explores the application of MoE in blind weather removal. We first introduce the MoE module into the ViT-based image restoration network and take it as our baseline. Although performance can be improved by introducing MoE directly, we still find two limitations of this baseline. Firstly, the basic router of MoE cannot well assign the correct

Y. Luo, R. Zhao, J. Chen, Y. Lu, T. Wang, R. Xiong, and S. Zhang are with Peking University, Beijing, China. (e-mail: {yulin, rui Zhao, 2000012967}@stu.pku.edu.cn, tianyuw2001@gmail.com, {cjlw, rqxiong, shanghang}@pku.edu.cn) (Corresponding author: Shanghang Zhang)

X. Wei is with University of Chinese Academy of Sciences, Beijing, China. (e-mail: weixiaobao0210@gmail.com)

S. Xie is with Wuhan University, Wuhan, China. (e-mail: xieshenghao@whu.edu.cn)

M. Lu is with Intel Labs China. Beijing, China. (e-mail: lu199192@gmail.com)

weather type to the input due to the coupled weather and content embedding. Secondly, since processing different weather types requires different receptive fields, naive experts fail to exploit the multi-scale features for better performance.

To this end, we propose a method called Weather-aware Multi-scale Mixture-of-Experts (WM-MoE) based on the Transformer for blind adverse weather removal. We use the vision transformer as the baseline, with a task-shared convolution head and tail, and a naive MoE module. To handle diverse adverse weather conditions with multiple weather experts, we design a WEather-Aware Router (WEAR) that can route each image token to specific experts based on decoupled content and weather features. Therefore, WEAR can focus more on weather information to select experts than image content such as texture richness and brightness. To obtain distinctive weather features, we propose Weather Guidance Fine-grained Contrastive Learning (WGF-CL). After obtaining weather tokens by a light-weight ViT encoder, WGF-CL optimizes the mutual distance of these embeddings in a token-level supervised contrastive learning manner, which utilizes the intra-weather similarity and inter-weather difference to guide the selection of positive and negative samples for each token. We further introduce Multi-Scale Experts (MSE) to fuse multi-scale features and enhance the spatial modeling capability, leading to better performance than the original token-wise FFN experts. We demonstrate the effectiveness of the proposed WM-MoE on multiple benchmarks. In the upstream blind weather removal task, WM-MoE surpasses current state-of-the-art (SOTA) methods on the proposed dataset MAWSim by PSNR +1.51 and SSIM +0.022, the public dataset Allweather [24] by PSNR +0.96 and SSIM +0.0304, RainCityscapes [33] by PSNR +0.31 and HazeCityscapes [34] by PSNR +1.58. In the downstream task, the image recovered by our method can also improve the performance of the semantic segmentation model, which is more stable than other methods. The contributions can be concluded as follows:

- We propose a novel framework named Weather-aware Multi-scale Mixture-of-Experts (WM-MoE) for blind adverse weather removal. We design a WEather-Aware Router (WEAR) to assign specific experts for each image token more effectively based on decoupled content and weather features. We also develop Multi-Scale Experts (MSE) to aggregate local and multi-scale features, improving spatial modeling capability.
- We propose Weather Guidance Fine-grained Contrastive Learning (WGF-CL) to capture discriminative and detailed weather representation. The learned weather features serve as supplementary input for WEAR to select experts, effectively handling complex weather conditions.
- We conduct comprehensive experiments on two public datasets and our dataset and achieve SOTA blind weather removal performance. We also demonstrate the advantage of our method on downstream segmentation tasks.

## II. RELATED WORK

### A. Adverse Weather Removal

Adverse weather removal has been explored over the past years. Related works can be divided into task-specific and task-

agnostic. The adverse weather mainly includes rain, snow, and haze. For task-specific methods, one network aims to deal with certain weather. Li et al. [3], Ren et al. [4], and Jiang et al. [2] remove rain based on progressively refining the image. Dong et al. [9] remove haze based on boosting and error feedback. GridDehazeNet [8] and FFA-Net [10] use attention operations for dehazing. Wu et al. [11] introduce contrastive learning to dehaze. DeSnowNet [17], JSTASR [18], and Chen et al. [19] aims to remove snow with different status adaptively.

In contrast to task-specific methods, some methods can be adopted for different weathers, i.e., the task-agnostic methods. Some of these methods can deal with only one type of degradation. These methods need to be trained for each task separately. MPRNet [20], SwinIR [21], and Restormer [22] are architectures for general image restoration. Most of these architectures implement deraining as one of the tasks in the experiments. Some methods can remove multiple adverse weathers at once. All-in-One [28] uses neural architecture search (NAS) to discriminate between different tasks. Several strategies are proposed to handle multiple adverse weathers simultaneously. TransWeather [24] uses learnable weather-type embeddings in the decoder. Chen et al. [35] use a two-stage knowledge-learning mechanism for comprehensive bad weather. BID [27] aims to decompose degraded images into constituent underlying images and other components.

### B. Transformer in Image Restoration Task

Transformers [36] have been increasingly applied in the vision area since ViT [37] employ Transformers to visual recognition task [29]. IPT [23] introduces Transformers pre-trained on a large dataset for image restoration tasks. SwinIR [21] introduces the Transformers with shifted windows [38] for image restoration. UFormer [39] and Restormer [22] use Transformers to construct pyramidal network structures for image restoration based on locally-enhanced windows and channel-wise self-attention, respectively. ELAN [40] and DATSR [41] consider long-range attention based on Transformers for super-resolution. CAT [42] and Xiao et al. [43] propose Transformers with adaptive windows to perform more flexible image restoration. Image De-raining Transformer (IDT) [44] develops the complementary window-based and spatial-based transformer to capture local and non-local features. Dehazeformer [45] explores the limitation of Swin Transformer [38] when applied to haze removal and proposes several improvements including modified normalization layer, activation function, and spatial information aggregation scheme. SnowFormer [46] employs cross-attention to model the local-global context interaction across patches for better desnowing.

### C. Mixture-of-Experts (MoE)

MoE is a type of neural network, whose parameters are partitioned into different subsets called "experts" [48]. Different parts of inputs will be routed to specific experts by some router mechanisms in training and inference time [48]. MoE was applied and popularized first in Natural Language Processing (NLP) in the deep learning era. It usually appears

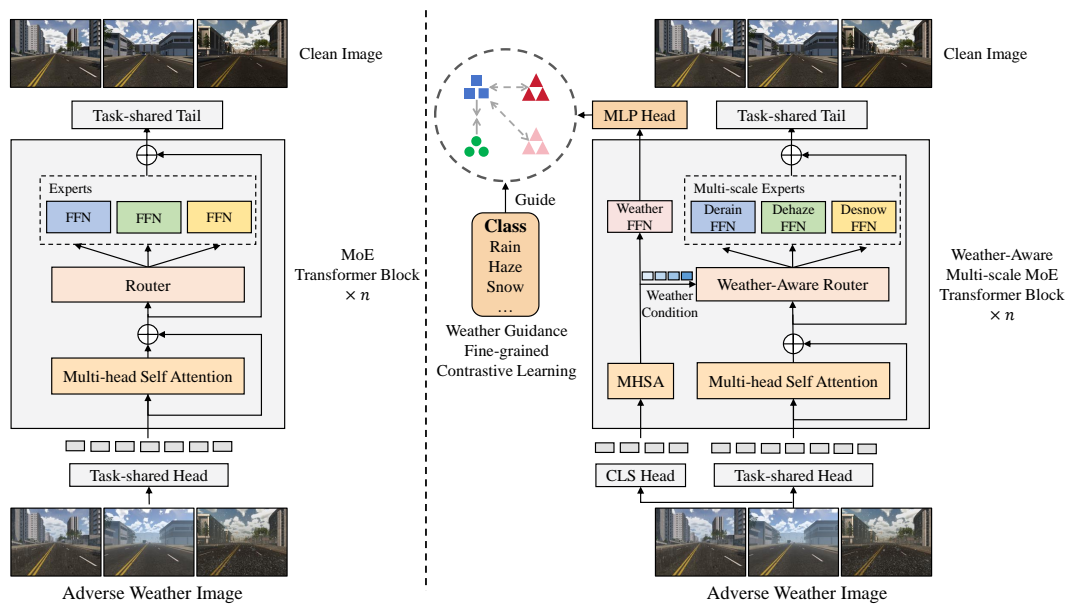


Fig. 1. Comparison between (a) naive Mixture-of-Experts (MoE) module [47] and (b) our proposed Weather-aware Multi-scale Mixture-of-Experts (WM-MoE) module. The linear layer router and point-wise FFN experts in the original MoE fail to deal with coupled content and weather features, and local information. Respectfully, we propose a Weather-aware Router to select experts dynamically based on decoupled content and weather embedding and Multi-scale Experts to make full use of local and multi-scale features.

as a basic model component, such as the expert FFN layers in Transformer [47], [49].

The primary purpose of MoE is to scale up model parameters to achieve better performance while maintaining high computation efficiency [48]. At the same time, the applications of MoE in multi-task learning and cross-domain learning are also explored. MMoE [50] utilizes multi-gate routing mechanism to model the relationship of different tasks. [51] introduces task-level routing instead of common-used token-level routing to realize more efficient inference. DEMix [52] introduces domain experts, each of them specialized in different language domains (e.g. medical, News, etc.) and could be ensembled to better generalize to unseen domains. All these works indicate the potential of MoE beyond scaling up.

In computer vision, MoE has been employed in some high-level tasks such as image classification [53], [54], object detection [54], [55] and segmentation [55]. MoE has also been used in low-level vision. Literature [56] and [57] extract underlying degradation features to construct MoE adaptive network to handle different degradation in blind super-resolution. HCT-FFN [30] uses MoE to learn spatially-varying rain distribution features in the deraining task. DRSformer [31] uses MoE to extract sparse content features from rainy images. DAN-Net [32] utilizes adaptive attention gate to modulate the outputs of task-specific experts to handle adverse winter weather conditions. Compared with works mentioned above, we focus on the blind adverse weather removal task. We first explore the limitation of the naive MoE structure when applied to this scenario from token assignment and multi-scale features extraction, and then propose specific MoE design to improve performance.

### III. PROPOSED APPROACH – WM-MOE

In this section, we first present the overall pipeline of our WM-MoE framework. Then we introduce the baseline,

naive MoE module in ViT, and analyze its limitation when applied to the task setting. Afterward, we provide the details of the proposed Weather-aware Multi-scale Mixture-of-Experts (WM-MoE), which includes several key components specially designed for blind weather removal tasks: Weather-aware Router, Weather Guidance Fine-grained Contrastive Learning and Multi-scale Experts.

#### A. Overall Framework

The overall pipeline of WM-MoE is shown in Fig.1 (b). WM-MoE has two parallel branches, one for obtaining weather representation efficiently, and the other for image restoration using task-related features. Both branches are based on Vision Transformer due to their ability in low-level visual tasks [22].

Given an image  $\mathbf{I}_{\text{adverse}} \in \mathbb{R}^{3 \times H \times W}$  with adverse weather, for the weather representation captured branch, we utilize ViT [37] to obtain patch-level weather embedding. Then we optimize Weather Guidance Fine-grained Contrastive Learning loss to achieve discriminative features, which is an additional input to Weather-aware Router in the restoration branch.

For the weather removal branch, we first obtain shallow image embeddings by a task-shared convolution head to capture low-level features. After applying patch embedding to image features, tokens are passed through Transformer encoder with  $L$  blocks. In each block, self-attention module models global relationships, followed by the proposed Weather-aware Multi-scale MoE module, which includes a Weather-aware Router to assign tokens reasonably and flexibly based on decoupled content and weather embeddings, and Multi-scale Experts to make full use of local and multi-scale information to handle weather with various conditions. After that, we employ a linear layer to expand token dimensions and reshape them to the origin resolution. Finally, a task-shared convolution tail is

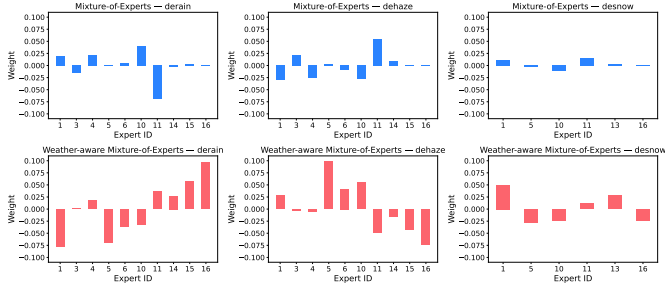


Fig. 2. Comparison of normalized routing scores histogram between MoE and Weather-aware Router (ours).

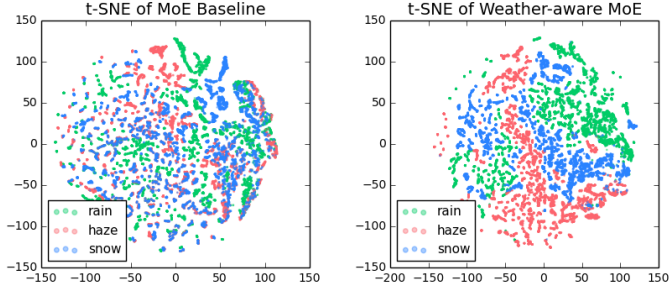


Fig. 3. Comparison of t-SNE of routing weights between MoE and Weather-aware Router (ours).

utilized to refine features and adjust channels to obtain the restoration clean image.

**B. Baseline: Mixture-of-Experts Module in ViT**

We first introduce our baseline, MoE in ViT, and then analyze its problems for blind weather removal tasks.

MoE baseline [49], [58] includes two parts. The experts consist of multiple parallel FFNs. The input tokens are passed through each expert and then fusion by weighted summation. Weights are generated by the router. It takes each token as input and outputs the probability of each token belonging to a specific expert. We choose Top-K experts for every token. Overall, the formulation of the naive MoE module can be summarized as follows:

$$g(\mathbf{y}^\ell) = \text{Softmax}(\text{Top-K}(\mathbf{W}\mathbf{y}^\ell)) \quad (1)$$

$$\mathbf{z}^{\ell+1} = \left[ \sum_{i=1}^M g_i(\mathbf{y}^\ell) \times \text{FFN}_i(\text{LN}(\mathbf{y}^\ell)) \right] + \mathbf{y}^\ell \quad (2)$$

where  $\mathbf{y}^\ell \in \mathbb{R}^{N \times D}$  is the output of self-attention module,  $\mathbf{z}^\ell \in \mathbb{R}^{N \times D}$  is the input tokens of  $\ell$ -th Transformer block,  $g(\mathbf{z}^\ell) \in \mathbb{R}^M$  is output weights of the router,  $g_i(\mathbf{z}^\ell)$  and  $\text{FFN}_i$  are the fusion weights and the  $i$ -th expert respectively, and  $M$  is the number of the task experts.

**C. Weather-aware Router**

In ideal conditions, experts will form different groups automatically with each one proficient in dealing with specific weather conditions with the help of a router with dynamic tokens routing mechanism.

To verify the hypothesis, we calculate the routing scores  $s_{i,w}$  by averaging the output weights of the router for each token from images with different weather types, where  $i$  is the ID of experts,  $w$  is the weather type including rain, haze, and snow. To compare  $s_{i,w}$  of different weather more clearly, we present the histogram of normalized routing scores  $s_{i,w}^{norm} = s_{i,w} - \sum_w s_{i,w}$  in Fig.2 (a). If the hypothesis is right, the variance of  $s_{i,w}^{norm}$  will be large. However, we observe normalized routing score almost tends to zero for all weather, which means there is no preference for the router to deal with different weather. We also visualize the t-SNE of the router’s weights for different weather in Fig.3 (a), which also matches the above conclusion because the t-SNE features are mixed together.

So we rethink the router designed in naive MoE. We find in fact it’s hard for the original router to select tokens according to weather conditions. The essence of the routing mechanism is to complete the pattern matching and clustering of tokens for each expert. In high-level tasks, different tokens contain abstract semantic features with high similarity [53], resulting in easier clustering. But in the blind weather removal task, the content and weather feature of patch embedding are coupled, making router difficult to select specific experts according to the content or weather information, which limits the assignment flexibility.

We analyze this is because the original router is hard to select tokens according to weather conditions due to the coupled content and weather features (details in supplementary material). In view of the current router’s drawback, we propose a Weather-aware Router to explicitly make use of the weather feature. In the training stage, we employ Weather Guidance Fine-grained Contrastive Learning to learn token-level weather features as the weather representation learning branch, which will be introduced in the next section.

These token-level weather embeddings could be used as a supplementary assignment basis for the router in the restoration branch. We concatenate weather tokens  $\mathbf{z}^l$  and content tokens  $\mathbf{y}^\ell$  along the channel dimension to obtain  $[\mathbf{y}^\ell, \mathbf{z}^l] \in \mathbb{R}^{N \times 2D}$ , and then utilize a nonlinear adaptor to aggregate the feature. The adaptor’s outputs are the final inputs of the router. The formulation can be summarized as follows:

$$g(\mathbf{y}^\ell, \mathbf{z}^L) = \text{Softmax}(\text{Top-K}(\text{Adaptor}([\mathbf{y}^\ell, \mathbf{z}^L])\mathbf{W})) \quad (3)$$

In this way, WEAR can select experts based on decoupled content and weather features, which is more flexible and leads to better performance. For WEAR, the normalized routing score has a larger variance and t-SNE features are more separated, shown in Fig. 2 and 3 (b) respectfully, demonstrating WEAR’s effectiveness.

**D. Weather Guidance Fine-grained Contrastive Learning**

Contrastive Learning (CL) has been explored for learning representation to modulate networks in low-level vision tasks. DASR [59] proposes unsupervised degradation contrastive learning (UDCL) for blind super-resolution (blind SR). UDCL follows a prior assumption, the low-resolution degradation is the same for the same image, and different

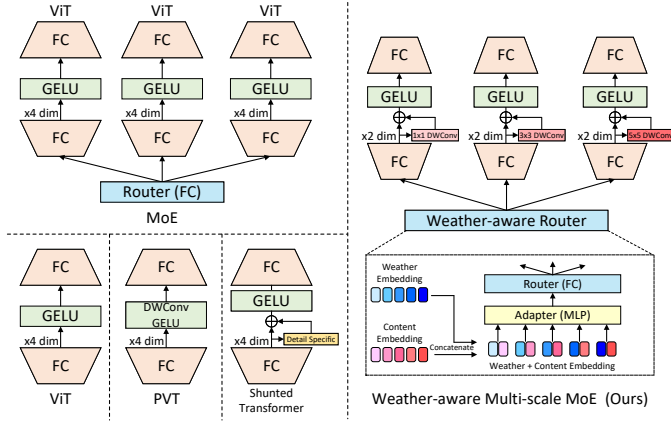


Fig. 4. Comparison of ViT [37], PVT [62], Shunted Transformer [63], MoE [49] and proposed Weather-aware Multi-scale MoE in terms of FFN module.

for different images, resulting in corresponding instance-level positive and negative samples. UDCL first randomly selects  $B$  low-resolution images and randomly crops two patches from each image, with patch embeddings  $p_i^1, p_i^2, i = 1, \dots, B$ . UDCL builds an online queue [60] to store negative samples  $p_{queue}^j, j = 1, \dots, N_{queue}$ . The formulation is as follows:

$$L_{udcl} = \sum_{i=1}^B -\log \frac{\exp(p_i^1 \cdot p_i^2 / \tau)}{\sum_{j=1}^{N_{queue}} \exp(p_i^1 \cdot p_{queue}^j / \tau)} \quad (4)$$

where  $\tau \in \mathbb{R}^+$  is a scalar temperature parameter.

Different from blind SR, the degradation in blind weather removal shows obvious group characteristics. A real weather image consists of some basic weather elements like rain streaks, raindrops, haze, and snowflakes. If we apply UDCL in blind weather, it's easy to get false negative examples. For example, patch embeddings from a rain image will be pushed to those from another rain image.

To better enable CL to learn blind weather features, motivated by Supervised Contrastive Learning (SCL) [61], which uses classification labels to avoid false negative samples, we propose Weather Guidance Fine-grained Contrastive Learning (WGF-CL) (Fig. 5). Though we can't obtain the weather type in test time, we can still utilize weather labels to help model training. SCL regards different augmented views (global features) of images with the same semantic label as positive samples, while WGF-CL regards all patch embeddings (local features) of images with the same weather as positive samples. The formulation is summarized as follows.

$$\mathbf{z}_i^L = \text{ViT}(\mathbf{I}_{\text{adverse}}) = [z_{i,1}^L, \dots, z_{i,j}^L, \dots, z_{i,N}^L] \quad (5)$$

$$L_{wgf-cl} = \sum_{i \in I} \frac{-1}{|P(i)|} \sum_{p \in P(i)} \log \frac{\exp(\mathbf{z}_i^L \cdot \mathbf{z}_p^L / \tau)}{\sum_{a \in A(i)} \exp(\mathbf{z}_i^L \cdot \mathbf{z}_a^L / \tau)} \quad (6)$$

where  $\mathbf{z}_i^L \in \mathbb{R}^{N \times D}$  is the output of the weather feature encoder,  $i \in I \equiv \{1, \dots, B\}$  is the index of minibatch,  $A(i) \equiv I \setminus \{i\}$ ,  $P(i) \equiv \{p \in A(i) : y_p = y_i\}$  is the positive samples group of the  $i$ -th anchor sample.

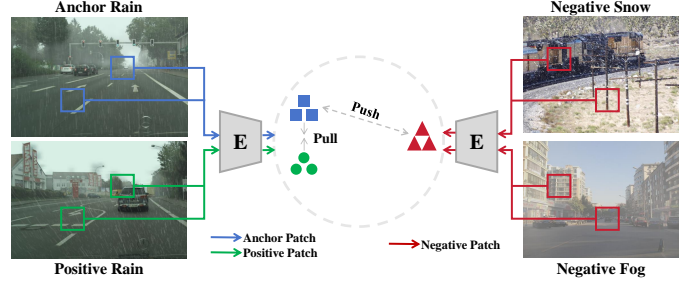


Fig. 5. The illustration of proposed Weather Guidance Fine-grained Contrastive Learning. Patch embeddings from images with the same weather are regarded as positive samples and from different weather are negative samples.

Compared to UDCL, WGF-CL utilizes weather prior information to guide contrastive learning to select appropriate positive samples and help to capture group-level weather representation.

### E. Multi-scale Experts

Different weather requires information on different receptive fields to deal with. For example, the occlusion is more serious in heavy rain, so the receptive field should be larger than in light rain for removal. However, the original MoE can only process token-level information due to point-wise FFN.

To this end, we design Multi-scale Experts (Fig. 4) to process information at different scales. Motivated by Inception [64], we propose grouping experts at different scales. Each expert has a parallel depth-wise convolution with  $n \times n$  kernel size, denoted as  $\text{DWConv}_n$ , and different groups have different  $n$ , where  $n \in \{1, 3, 5, 7\}$ . The formulations are as follows:

$$\mathbf{z}^{\ell+1} = \left[ \sum_{i=1}^M g_i(\mathbf{y}^\ell) \times \text{FFN}_{MS,i}(\text{LN}(\mathbf{y}^\ell)) \right] + \mathbf{y}^\ell \quad (7)$$

$$\text{FFN}_{MS,i}(\mathbf{x}) = \text{FC}(\sigma(\text{FC}(\mathbf{x}) + \text{DWConv}_n(\text{FC}(\mathbf{x})))) \quad (8)$$

Where  $\text{FFN}_{MS,i}$  is the  $i$ -th multi-scale expert, FC is the fully connected layer, and  $\sigma$  is GELU. Combined with WEAR, the model can adaptively select experts with appropriate receptive fields to process different weather conditions.

### F. Loss Function

We use the smooth-L1 loss and perceptual loss [65] for the restoration branch and weather guidance fine-grained contrastive learning (WGF-CL) loss for the weather representation learning branch. For perceptual loss, we extract features from the 3<sup>rd</sup>, 8<sup>th</sup> and 15<sup>th</sup> layers of VGG16 [66] pretrained on ImageNet and calculate the MSE of features from the restored image and GT. For WGF-CL loss, we set  $\tau = 2$ . The overall loss can be summarized as follows:

$$L_{total} = L_{smooth-L1} + \lambda_1 L_{perceptual} + \lambda_2 L_{WGF-CL} \quad (9)$$

where  $\lambda_1 = 0.04$  and  $\lambda_2 = 0.01$ .





Fig. 6. Examples of MAW-Sim visualizations. We provide pair of RGB images in 4 weather types. (Best view on screen)

TABLE I  
QUANTITATIVE COMPARISON ON ALL-WEATHER DATASET. THE GMACS AND TIME ARE TESTED ON  $256 \times 256$  IMAGES.

Type	Method	Derain	Deraindrop	Desnow	Average	Params (M)	GMacs	Time (ms)	
		PSNR / SSIM	PSNR / SSIM	PSNR / SSIM	PSNR / SSIM				
Task Specific	Derain	RESCAN [3]	21.57 / 0.7255	24.26 / 0.8367	24.30 / 0.7586	23.38 / 0.7736	0.15	32.32	26.5
		PRENet [4]	23.16 / 0.8624	24.96 / 0.8629	25.19 / 0.8483	24.44 / 0.8579	0.17	66.58	23.0
	Dehaze	GridDehazeNet [8]	25.31 / 0.8657	27.32 / 0.8723	27.19 / 0.8457	26.61 / 0.8612	0.96	21.49	21.2
		MSBDN-DFF [9]	22.62 / 0.8217	21.22 / 0.8189	25.46 / 0.8130	23.10 / 0.8179	28.71	24.61	45.0
		FFA-Net [10]	27.96 / 0.8857	27.73 / 0.8894	27.21 / 0.8578	27.63 / 0.8776	4.46	288.34	55.9
		AECR-Net [11]	26.77 / 0.8493	26.54 / 0.8846	26.77 / 0.8509	26.70 / 0.8616	2.61	43.07	10.0
	Desnow	DesnowNet [17]	12.73 / 0.5327	23.80 / 0.8440	21.89 / 0.7682	19.47 / 0.7150	26.15	107.32	69.2
		HDCWNet [19]	14.59 / 0.6314	24.51 / 0.8514	20.21 / 0.7447	19.77 / 0.7425	6.99	—	—
	Task Agnostic	MPR [20]	<b>28.35 / 0.9100</b>	<b>28.33 / 0.9063</b>	27.77 / 0.8772	<b>28.15 / 0.8978</b>	3.64	148.55	63.5
Restormer [22]		27.85 / 0.8802	28.32 / 0.8881	<b>28.18 / 0.8684</b>	28.12 / 0.8789	26.13	140.99	65.4	
Multi Task in One	Transweather [24]	25.64 / 0.8103	27.37 / 0.8570	26.98 / 0.8305	26.66 / 0.8326	38.05	6.12	28.3	
	Unified Model [35]	25.81 / 0.8544	<b>28.33 / 0.8832</b>	27.94 / 0.8679	27.36 / 0.8685	28.71	24.61	42.2	
	<b>WM-MoE (All-Weather)</b>	<b>28.59 / 0.9432</b>	<b>29.37 / 0.9400</b>	<b>29.37 / 0.9014</b>	<b>29.11 / 0.9282</b>	19.58	53.31	22.9	
	<b>WM-MoE (Maw-Sim + Cityscapes)</b>	—	—	—	—	17.47	51.27	21.2	

#### IV. EXPERIMENTS

In this section, we evaluate our work on MAW-Sim, All-Weather, and Cityscapes datasets and compare it with several SOTA methods. We also provide the performance comparison of downstream segmentation tasks in Cityscapes. Moreover, we implement an ablation study to demonstrate the effectiveness of each component of WM-MoE.

##### A. Experiment Setting

**MAW-Sim.** In order to train models for blind adverse weather removal, we collect and annotate a simulated dataset with multiple adverse weathers named *MAW-Sim*. It’s generated based on the Unity3D engine with a large city traffic system and a weather generation system. The images are recorded with a virtual camera on cars at 30fps. The dataset has 30 scenes. Each scene has 5 different cases, including clear day as ground truth, rain, snow, fog, and a random mix of them. Each scene has 30 frames with  $1024 \times 768$  resolution. We further divide the dataset for training, validation, and testing according to the ratio of 7:1:2.

**Dataset.** We evaluate WM-MoE and state-of-the-art methods on MAW-Sim, All-weather, and Cityscapes datasets. All-weather [24] contains data from different public datasets. The training set consists of Outdoor-Rain [67], Raindrop [68] and Snow100K [69]. The test set is sampled from Outdoor-Rain [67], the Raindrop test set [68], and the Snow 100k-L test set [69]. Cityscapes [70] is collected from various

scenarios of outdoor street scenes in different cities. These images are recorded in normal weather conditions by video cameras mounted on cars. Foggy Cityscapes [34] and Rain Cityscapes [33] are synthesized from the images in the Cityscapes dataset. We further combine the train sets of them for training. We also adopt the fine segmentation label of Cityscapes for downstream tasks evaluation.

TABLE II  
SUMMARY OF THE PROPOSED MAW-SIM DATASETS. WE COUNT THE NUMBER OF IMAGES IN THE TRAIN, VAL, AND TEST SETS OF DIFFERENT WEATHER TYPES IN THE DATASETS. MIX REPRESENTS THE MIX OF THE RAINY, SNOWY, AND FOGGY WEATHER TYPES.

MAW-Sim	Train	Validation	Test
Rainy	0.84K	0.12K	0.24K
Snowy	0.84K	0.12K	0.24K
Foggy	0.84K	0.12K	0.24K
Mix	0.84K	0.12K	0.24K
Clear	0.84K	0.12K	0.24K
Total	4.2K	0.12K	0.24K

**Implementation Details.** WM-MoE is trained for 200 epochs with 32 batch sizes. We adopt the AdamW optimizer and Cosine scheduler with initial learning rates  $2e-4$  gradually reduced to  $2e-6$  and the warm-up strategy for 3 epochs. We randomly crop images to  $256 \times 256$  for training and apply a non-overlap crop for the same patch size in the test. For data augmentation, we use random flips and rotations.

TABLE III  
QUANTITATIVE COMPARISON ON MAW-SIM DATASET.

Type		Method	Derain	Dehaze	Desnow	Mixed Weather	Average
			PSNR / SSIM	PSNR / SSIM	PSNR / SSIM	PSNR / SSIM	PSNR / SSIM
Task Specific	Derain	RESCAN [3]	21.42 / 0.7467	22.30 / 0.8554	21.58 / 0.7177	20.77 / 0.6539	21.52 / 0.7434
		PReNet [4]	28.89 / 0.9170	29.47 / <b>0.9467</b>	<b>29.24 / 0.9330</b>	28.09 / <b>0.9081</b>	28.17 / <b>0.9262</b>
	Dehaze	GridDehazeNet [8]	28.96 / 0.8901	28.94 / 0.9216	29.22 / 0.9045	<b>28.21 / 0.8759</b>	28.83 / 0.8980
		MSBDN-DFE [9]	28.09 / 0.8985	28.55 / 0.9321	28.30 / 0.9118	27.48 / 0.8854	28.11 / 0.9070
		FFA-Net [10]	27.44 / 0.8776	28.73 / 0.9330	27.54 / 0.8810	26.30 / 0.8454	27.50 / 0.8843
		AECR-Net [11]	26.89 / 0.8584	27.76 / 0.9062	26.89 / 0.8658	26.29 / 0.8365	26.96 / 0.8667
	Desnow	DesnowNet [17]	20.51 / 0.6663	25.01 / 0.8352	20.16 / 0.6198	18.25 / 0.5446	20.98 / 0.6665
HDCWNet [19]		23.98 / 0.7236	25.42 / 0.8392	24.36 / 0.8254	21.36 / 0.6724	23.78 / 0.7652	
Task Agnostic	MPR [20]	27.02 / 0.8881	28.14 / 0.9297	27.81 / 0.9170	26.39 / 0.8753	27.34 / 0.9025	
	Restormer [22]	28.23 / 0.9016	28.21 / 0.9350	28.30 / 0.9137	27.11 / 0.8859	27.96 / 0.9091	
Multi Task in One	Transweather [24]	22.55 / 0.6608	22.97 / 0.7163	21.90 / 0.5857	21.38 / 0.5507	22.20 / 0.6284	
	Unified Model [35]	<b>29.04 / 0.8913</b>	<b>29.63 / 0.9312</b>	29.11 / 0.9002	28.00 / 0.8701	<b>28.95 / 0.8982</b>	
	<b>WM-MoE</b>	<b>30.38 / 0.9423</b>	<b>31.16 / 0.9656</b>	<b>30.77 / 0.9522</b>	<b>29.52 / 0.9328</b>	<b>30.46 / 0.9482</b>	

TABLE IV  
QUANTITATIVE COMPARISON ON CITYSCAPES.

Type		Method	Derain				Dehaze			
			Upstream		Downstream		Upstream		Downstream	
			PSNR $\uparrow$	SSIM $\uparrow$	mIoU $\uparrow$	mAcc $\uparrow$	PSNR $\uparrow$	SSIM $\uparrow$	mIoU $\uparrow$	mAcc $\uparrow$
Task Specific	Derain	RESCAN [3]	19.11	0.9118	0.1007	0.2064	16.96	0.9033	0.1262	0.2116
		PReNet [4]	19.95	0.8822	0.1321	0.2943	18.22	0.8729	0.3305	0.2508
	Dehaze	GridDehazeNet [8]	22.08	0.9171	0.4259	0.6945	23.18	0.9183	0.4453	0.7108
		MSBDN-DFE [9]	26.26	0.8853	0.1744	0.2733	26.79	0.8903	0.3426	0.4019
		FFA-Net [10]	28.29	0.9411	0.3458	0.5799	28.96	0.9432	0.4257	0.6005
		AECR-Net [11]	26.27	0.9075	0.2230	0.3516	27.75	0.9062	0.3714	0.4652
Task Agnostic	MPR [20]	<b>32.68</b>	<b>0.9810</b>	<b>0.4657</b>	<b>0.7580</b>	<b>29.73</b>	<b>0.9752</b>	<b>0.4537</b>	<b>0.7301</b>	
	Restormer [22]	28.06	0.9630	0.4383	0.6833	22.72	0.9411	0.4085	0.6920	
Multi Task in One	Transweather [24]	24.08	0.8481	0.4425	0.671	22.56	0.8736	0.3643	0.6105	
	Unified Model [35]	28.25	0.9504	0.4190	0.7246	27.96	0.9167	0.4336	0.7231	
	<b>WM-MoE</b>	<b>32.99</b>	<b>0.9755</b>	<b>0.4686</b>	<b>0.7701</b>	<b>31.31</b>	<b>0.9647</b>	<b>0.4545</b>	<b>0.7473</b>	
Lower Bound				0.3416	0.6020			0.4250	0.6391	
Upper Bound				0.4594	0.7685			0.4594	0.7685	

B. Network Details

**Task-shared Head.** We adopt a similar head setting as IPT [23], which consists of one convolution layer and two residual blocks. The former parameters are  $3 \times 3$  kernel size, 3 input channels, and 32 output channels. The latter block consists of a shortcut and parallel two convolution layers with  $3 \times 3$  kernel size, 32 input channels, and 32 output channels. The spatial resolution of feature maps remains unchanged in the process.

**Transformer Encoder.** We first obtain the patch embedding from feature maps by a non-overlap convolution projection and flatten operation. We set the dimension  $D$  to 256, 384 and 256 for MAW-Sim, Allweather [24] and Cityscapes [33], [34] respectively. The resultant sequence  $[B, N, D]$  is the input of Transformer, where  $B$  is the batch size,  $N$  is the number of patches and  $D$  is the embedding dimension.

For the restoration branch, the number of Transformer blocks is 2. In each block, standard multi-head self-attention module with 8 heads is adopted. The weather-aware token-level router consists of one linear layer and softmax function with  $2 \times D$  and  $E$  as input and output channels, where  $E$  denotes the number of experts. Before getting into the router, we adopt an adaptor with a two-layer MLP to process the concatenation of the content and weather token embeddings.  $E$  multi-scale experts are employed and divided into 4 groups,

with  $1 \times 1$ ,  $3 \times 3$ ,  $5 \times 5$  and  $7 \times 7$  for their bypass depth-wise convolution layer respectfully. To reduce the parameters and flops, the hidden layer dimension of each expert is set to  $2D$  instead of commonly used  $4D$  [37], [58].

For the weather representation captured branch, we use ViT [37] with 2 blocks, including multi-head self-attention module, and feed-forward network. All settings are the same as the restoration branch.

**Task-shared Tail.** The task-shared tail consists of 4 sequential blocks to adjust the channels of feature maps reconstructed from the Transformer output. The residual block and convolution layer are used twice alternately. The input channels are 128 and the output channels of each layer are 128, 64, 64, 3 respectively.  $3 \times 3$  kernel size is adopted for all of them. In the end, We utilize the Sigmoid function to normalize the final output in the range of 0 to 1.

C. Comparison with State-of-the-art Methods

**Baselines.** We compare our WM-MoE with task-specific, task-agnostic, and multi-task-in-one methods. Task-specific group includes derain (RESCAN [3] and PReNet [4]), dehaze (GridDehazeNet [8], MSBDN-DFE [9], FFA-Net [10], and AECR-Net [11]), and desnow (DesnowNet [17] and HDCWNet [19]). Task-agnostic group includes MPR [20], and Restormer [22]. The multi-task-in-one group includes Transweather [24] and Unified Model [35]. We retrain the models

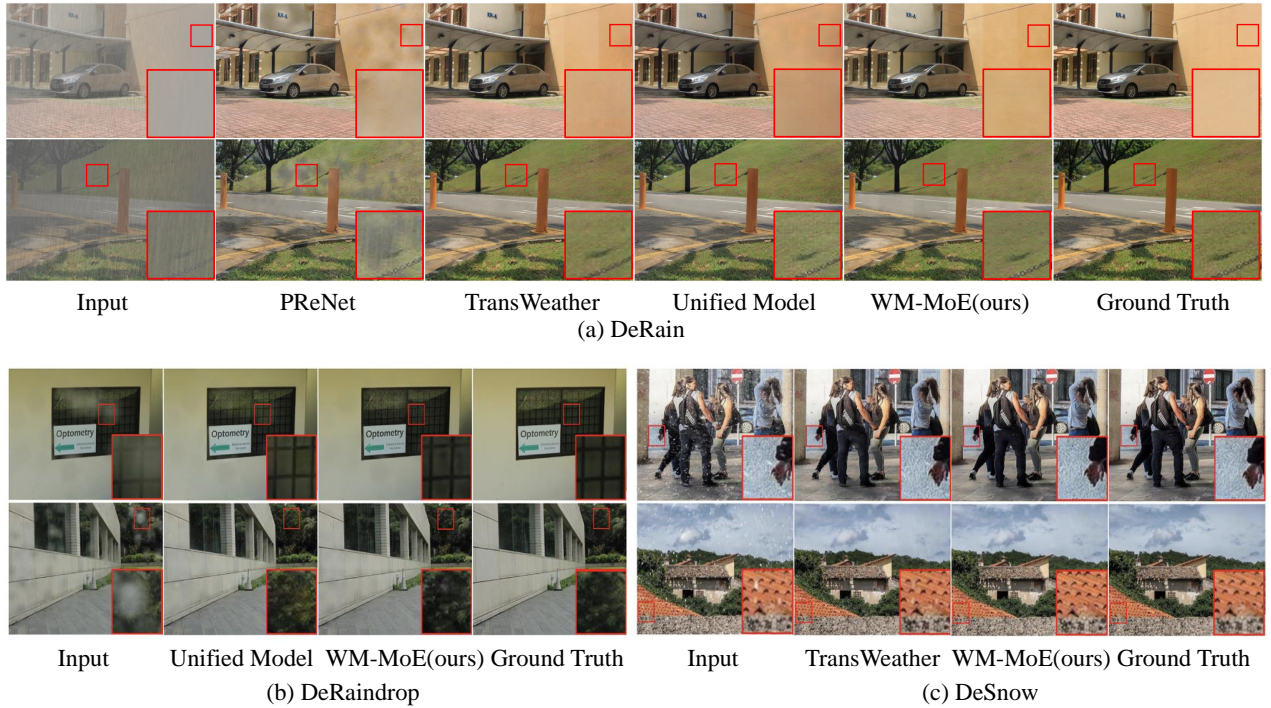


Fig. 7. Qualitative results to visualize the deweather performance on All-Weather.

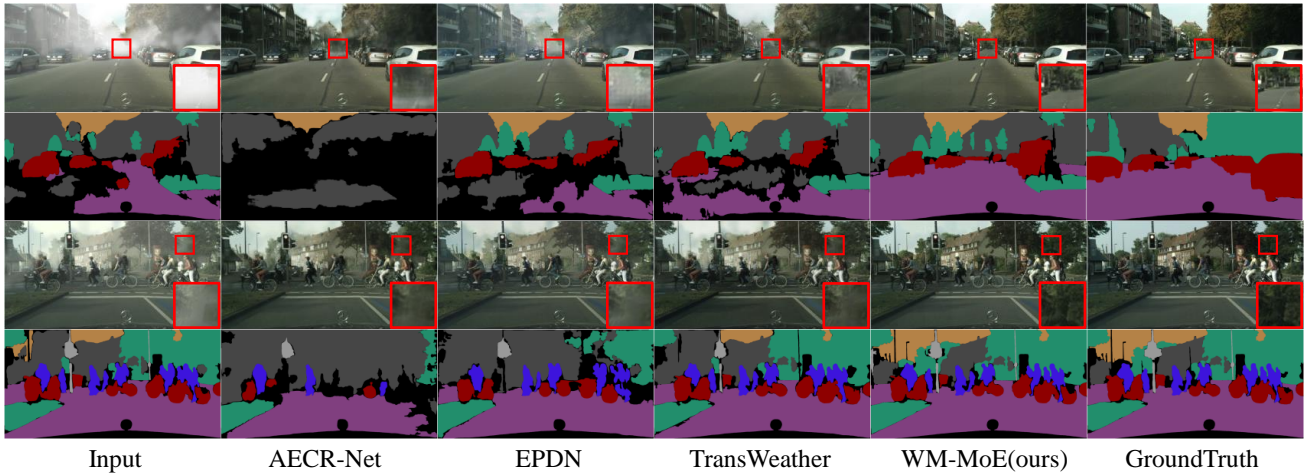


Fig. 8. Qualitative results of the deweather performance and downstream semantic segmentation on Cityscapes.

TABLE V  
ABLATION STUDIES ON WM-MoE. N IS THE NUMBER OF EXPERTS AND K IT THE TOPK GATE.

Baseline	Moe-Token	Weather-aware router	Multi-scale experts	Parameters (M)		Flops(G)		PSNR		SSIM	
				n4-k4	n16-k4	n4-k4	n16-k4	n4-k4	n16-k4	n4-k4	n16-k4
✓				4.95		71.96		29.51		0.9365	
✓	✓			6.53	12.86	75.20	88.12	29.69	29.84	0.9400	0.9420
✓	✓	✓		10.78	17.11	88.88	101.82	29.80	29.99	0.9406	0.9439
✓	✓	✓	✓	10.87	17.47	89.06	102.54	30.18	30.33	0.9441	0.9467

using open-source code. For downstream tasks, we implement experiments of the lower and upper bound, which take weather and clean images as downstream input respectively.

**Metrics.** For the quantitative evaluation of blind weather removal, we adopt PSNR and SSIM as metrics. We calculate the metrics in RGB space. For downstream semantic segmentation

tasks, we take mIoU, and mAcc as our metrics.

1) *Quantitative Comparison and Analysis:*

**Main results.** We report several weather and the average results in Tables I, III, and IV. It can be noted that our method achieves SOTA performances on both MAW-Sim and All-weather. WM-MoE also obtains competitive results on



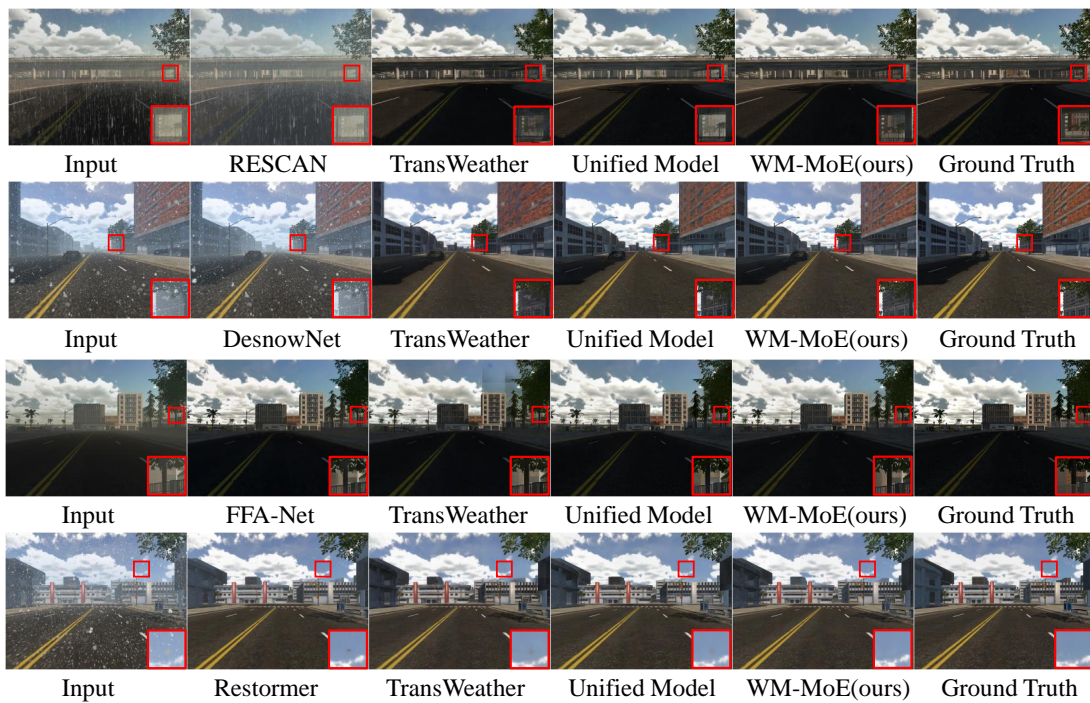


Fig. 9. Qualitative results to visualize the deweather performance on MAW-Sim.

TABLE VI

ABLATION STUDY ON THE PROPOSED WEATHER-AWARE MULTI-SCALE MIXTURE-OF-EXPERTS MODULE IN THE MAWSIM DATASET, INCLUDING THE NUMBER OF EXPERTS AND THE TOPK ROUTER. K=1 & N=1 REPRESENTS OUR BASELINE WITHOUT MOE MODULE

K / N	1		4		8		16		32	
	PSNR	SSIM	PSNR	SSIM	PSNR	SSIM	PSNR	SSIM	PSNR	SSIM
1	29.51	0.9365	29.65	0.9387	29.60	0.9383	29.63	0.9387	29.70	0.9395
2	\	\	29.98	0.9427	30.04	0.9440	30.03	0.9449	30.12	0.9445
3	\	\	29.91	0.9423	30.09	0.9446	30.25	0.9462	30.30	0.9461
4	\	\	30.09	0.9439	30.24	0.9454	30.29	0.9468	30.31	0.9467

TABLE VII

ABLATION STUDIES ON REPRESENTATION LEARNING.

Representation Learning Method	PSNR		SSIM	
	n4-k4	n16-k4	n4-k4	n16-k4
Classification	30.10	30.28	0.9439	0.9466
UDCL	29.98	30.25	0.9436	0.9468
WGF-CL	30.18	30.33	0.9441	0.9467

Cityscapes. For task-specific methods designed for specific deweather tasks, WM-MoE outperforms all of them by a significant margin. Compared with task-agnostic methods, our method also achieves more promising results, especially in mixed weather. In addition, our method still performs better than another multi-task in one work, regardless of scenario and weather conditions. Thanks to the Weather-aware Router and Multi-scale Experts, the model enhances the capacity to process complex weather conditions and exploit multi-scale features, which handles blind weather better.

**Downstream results.** As for downstream results in Tables IV, it can be seen that weather removal benefits segmentation tasks. WM-MoE achieves competitive results on deweather tasks while helping the downstream model obtain promising results, which is close to the upper bound performance.

#### D. Ablation Study

**Ablations on proposed modules.** We evaluate the contribution of each component to our method (Table V). The baseline is a vision Transformer with task-shared convolution head and tail. First, we replace the original FFN with naive MoE. Then we verify the WEAR to replace the linear layer router and the ME to replace point-wise FFN experts, respectively. Here we present two parameters of the number of experts  $n$  and TopK gate  $k$ . More ablations about  $n$  and  $k$  are in the supplementary material. All the ablations are conducted in MAW-Sim. The training settings are the same as Table III. It’s been shown that every design in WM-MoE could lead to a performance gain.

**Ablations on representation learning methods.** We also compare different representation learning methods (Table VII). WGF-CL achieves the best performance. It’s worth noting that the result of UDCL drops obviously, proving the hypothesis that instance-level CL against group characteristics in blind weather results in false negative samples.

**Ablations on the number of experts and top-k gate.** We present more ablation experiments on different N & K in the MAW-Sim dataset with the same training setting as the main experiments. The concrete value of PSNR and SSIM is in Table VI and the corresponding line chart is in Figure 11.



Fig. 10. Qualitative results to visualize the downstream semantic segmentation performance on MAW-Sim.

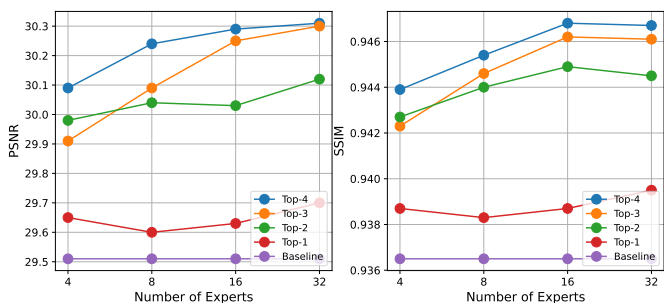


Fig. 11. Ablation study on the proposed Weather-aware Multi-scale Mixture-of-Experts Module. The same results with Table VI

From the Table VI and Figure 11, we can summarize the following conclusion:

(1) The proposed MoE module can improve the baseline consistently, whatever  $N$  or  $K$  is.

(2) When  $K$  is fixed, the performance is guaranteed to go up with  $N$  increasing from 4 to 32, and the PSNR- $N$  growth curve is close to a logistics curve like the formulation of PSNR, which demonstrates the scaling ability of MoE. Due to limited computing resources, we don't explore more experts, but we will take it as the direction for future improvements.

(3) For  $K=1$ , the performance increase unsteadily. We think this is because smaller  $K$  and larger  $N$  make each expert get fewer tokens to obtain strong capacity when the trainset and training time are limited.

(3) When  $N$  is fixed, larger  $K$  brings about better performance while more computation at the same time because  $K$  controls the sparsity of MoE module [58], [71].

After considering the overall performance and efficiency, we choose  $N = 16$  &  $K = 4$  as the final version.

## V. CONCLUSION

In this work, we study the blind weather removal problem. To better release the potential of MoE in the setting, we propose a novel Weather-aware Multi-scale MoE (WM-MoE), which consists of the Weather-aware Router (WEAR) to assign the correct weather experts to tokens and Multi-scale Experts (ME) to improve the spatial modeling capability. We also propose Weather Guidance Fine-grained Contrastive Learning (WGF-CL) to decouple the weather and content information from the input image. Our method achieves SOTA performance in MAW-Sim, All-Weather, and competitive results in Cityscapes. Experiments also demonstrate that WM-MoE is beneficial to the downstream segmentation task.

## REFERENCES

- [1] H. Liu, Y. Sun, Y. Bandoh, M. Kitahara, and S. Satoh, "Deep counterfactual representation learning for visual recognition against weather corruptions," *IEEE Trans. Multimedia*, 2023.
- [2] K. Jiang, Z. Wang, P. Yi, C. Chen, B. Huang, Y. Luo, J. Ma, and J. Jiang, "Multi-scale progressive fusion network for single image deraining," in *IEEE Conf. Comput. Vis. Pattern Recog.*, 2020, pp. 8346–8355.
- [3] X. Li, J. Wu, Z. Lin, H. Liu, and H. Zha, "Recurrent squeeze-and-excitation context aggregation net for single image deraining," in *Eur. Conf. Comput. Vis.*, 2018, pp. 254–269.
- [4] D. Ren, W. Zuo, Q. Hu, P. Zhu, and D. Meng, "Progressive image deraining networks: A better and simpler baseline," in *IEEE Conf. Comput. Vis. Pattern Recog.*, 2019, pp. 3937–3946.
- [5] L. Yu, B. Wang, J. He, G.-S. Xia, and W. Yang, "Single image deraining with continuous rain density estimation," *IEEE Trans. Multimedia*, vol. 25, pp. 443–456, 2021.
- [6] Y. Yang, J. Guan, S. Huang, W. Wan, Y. Xu, and J. Liu, "End-to-end rain removal network based on progressive residual detail supplement," *IEEE Trans. Multimedia*, vol. 24, pp. 1622–1636, 2021.
- [7] Y. Wang, D. Gong, J. Yang, Q. Shi, D. Xie, B. Zeng *et al.*, "Deep single image deraining via modeling haze-like effect," *IEEE Trans. Multimedia*, vol. 23, pp. 2481–2492, 2020.
- [8] X. Liu, Y. Ma, Z. Shi, and J. Chen, "Griddehazenet: Attention-based multi-scale network for image dehazing," in *Int. Conf. Comput. Vis.*, 2019, pp. 7314–7323.
- [9] H. Dong, J. Pan, L. Xiang, Z. Hu, X. Zhang, F. Wang, and M.-H. Yang, "Multi-scale boosted dehazing network with dense feature fusion," in *IEEE Conf. Comput. Vis. Pattern Recog.*, 2020, pp. 2157–2167.
- [10] X. Qin, Z. Wang, Y. Bai, X. Xie, and H. Jia, "Ffa-net: Feature fusion attention network for single image dehazing," in *AAAI Conf. Artif. Intell.*, vol. 34, 2020, pp. 11 908–11 915.
- [11] H. Wu, Y. Qu, S. Lin, J. Zhou, R. Qiao, Z. Zhang, Y. Xie, and L. Ma, "Contrastive learning for compact single image dehazing," in *IEEE Conf. Comput. Vis. Pattern Recog.*, 2021, pp. 10 551–10 560.
- [12] J. Li, Y. Li, L. Zhuo, L. Kuang, and T. Yu, "Usid-net: Unsupervised single image dehazing network via disentangled representations," *IEEE Trans. Multimedia*, 2022.
- [13] C. Lin, X. Rong, and X. Yu, "Msaff-net: Multiscale attention feature fusion networks for single image dehazing and beyond," *IEEE Trans. Multimedia*, 2022.
- [14] J. Shin, H. Park, and J. Paik, "Region-based dehazing via dual-supervised triple-convolutional network," *IEEE Trans. Multimedia*, vol. 24, pp. 245–260, 2021.
- [15] H.-M. Hu, H. Zhang, Z. Zhao, B. Li, and J. Zheng, "Adaptive single image dehazing using joint local-global illumination adjustment," *IEEE Trans. Multimedia*, vol. 22, no. 6, pp. 1485–1495, 2019.
- [16] Y. Song, J. Li, X. Wang, and X. Chen, "Single image dehazing using ranking convolutional neural network," *IEEE Trans. Multimedia*, vol. 20, no. 6, pp. 1548–1560, 2017.
- [17] Y.-F. Liu, D.-W. Jaw, S.-C. Huang, and J.-N. Hwang, "Desnownet: Context-aware deep network for snow removal," *IEEE Trans. Image Process.*, vol. 27, no. 6, pp. 3064–3073, 2018.
- [18] W.-T. Chen, H.-Y. Fang, J.-J. Ding, C.-C. Tsai, and S.-Y. Kuo, "Jstasr: Joint size and transparency-aware snow removal algorithm based on modified partial convolution and veiling effect removal," in *Eur. Conf. Comput. Vis.*, 2020, pp. 754–770.
- [19] W.-T. Chen, H.-Y. Fang, C.-L. Hsieh, C.-C. Tsai, I. Chen, J.-J. Ding, S.-Y. Kuo *et al.*, "All snow removed: Single image desnowing algorithm using hierarchical dual-tree complex wavelet representation and contradict channel loss," in *Int. Conf. Comput. Vis.*, 2021, pp. 4196–4205.
- [20] S. W. Zamir, A. Arora, S. Khan, M. Hayat, F. S. Khan, M.-H. Yang, and L. Shao, "Multi-stage progressive image restoration," in *IEEE Conf. Comput. Vis. Pattern Recog.*, 2021, pp. 14 821–14 831.
- [21] J. Liang, J. Cao, G. Sun, K. Zhang, L. Van Gool, and R. Timofte, "Swinir: Image restoration using swin transformer," in *Int. Conf. Comput. Vis. Workshops*, 2021, pp. 1833–1844.
- [22] S. W. Zamir, A. Arora, S. Khan, M. Hayat, F. S. Khan, and M.-H. Yang, "Restormer: Efficient transformer for high-resolution image restoration," in *IEEE Conf. Comput. Vis. Pattern Recog.*, 2022, pp. 5728–5739.
- [23] H. Chen, Y. Wang, T. Guo, C. Xu, Y. Deng, Z. Liu, S. Ma, C. Xu, C. Xu, and W. Gao, "Pre-trained image processing transformer," in *IEEE Conf. Comput. Vis. Pattern Recog.*, 2021, pp. 12 299–12 310.
- [24] e. a. Valanarasu, "Transweather: Transformer-based restoration of images degraded by adverse weather conditions," in *IEEE Conf. Comput. Vis. Pattern Recog.*, 2022, pp. 2353–2363.
- [25] W.-T. Chen, Z.-K. Huang, C.-C. Tsai, H.-H. Yang, J.-J. Ding, and S.-Y. Kuo, "Learning multiple adverse weather removal via two-stage knowledge learning and multi-contrastive regularization: Toward a unified model," in *IEEE Conf. Comput. Vis. Pattern Recog.*, 2022, pp. 17 653–17 662.
- [26] A. Kulkarni, P. W. Patil, S. Murala, and S. Gupta, "Unified multi-weather visibility restoration," *IEEE Trans. Multimedia*, 2022.
- [27] J. Han, W. Li, P. Fang, C. Sun, J. Hong, M. A. Armin, L. Petersson, and H. Li, "Blind image decomposition," in *Eur. Conf. Comput. Vis.*, 2022, pp. 218–237.
- [28] R. Li, R. T. Tan, and L.-F. Cheong, "All in one bad weather removal using architectural search," in *IEEE Conf. Comput. Vis. Pattern Recog.*, 2020, pp. 3175–3185.
- [29] K. Han, Y. Wang, H. Chen, X. Chen, J. Guo, Z. Liu, Y. Tang, A. Xiao, C. Xu, Y. Xu *et al.*, "A survey on vision transformer," *IEEE Trans. Pattern Anal. Mach. Intell.*, 2022.
- [30] X. Chen, J. Pan, J. Lu, Z. Fan, and H. Li, "Hybrid cnn-transformer feature fusion for single image deraining," in *AAAI Conf. Artif. Intell.*, 2023, pp. 378–386.
- [31] X. Chen, H. Li, M. Li, and J. Pan, "Learning a sparse transformer network for effective image deraining," in *IEEE Conf. Comput. Vis. Pattern Recog.*, 2023, pp. 5896–5905.
- [32] T. Ye, S. Chen, Y. Liu, E. Chen, and Y. Li, "Towards efficient single image dehazing and desnowing," *arXiv preprint arXiv:2204.08899*, 2022.
- [33] X. Hu, C.-W. Fu, L. Zhu, and P.-A. Heng, "Depth-attentional features for single-image rain removal," in *IEEE Conf. Comput. Vis. Pattern Recog.*, 2019, pp. 8022–8031.
- [34] C. Sakaridis, D. Dai, S. Hecker, and L. Van Gool, "Model adaptation with synthetic and real data for semantic dense foggy scene understanding," in *Eur. Conf. Comput. Vis.*, 2018, pp. 687–704.
- [35] W.-T. Chen, Z.-K. Huang, C.-C. Tsai, H.-H. Yang, J.-J. Ding, and S.-Y. Kuo, "Learning multiple adverse weather removal via two-stage knowledge learning and multi-contrastive regularization: Toward a unified model," in *IEEE Conf. Comput. Vis. Pattern Recog.*, 2022, pp. 17 653–17 662.
- [36] A. Vaswani, N. Shazeer, N. Parmar, J. Uszkoreit, L. Jones, A. N. Gomez, L. Kaiser, and I. Polosukhin, "Attention is all you need," *Adv. Neural Inform. Process. Syst.*, vol. 30, 2017.
- [37] A. Dosovitskiy, L. Beyer, A. Kolesnikov, D. Weissenborn, X. Zhai, T. Unterthiner, M. Dehghani, M. Minderer, G. Heigold, S. Gelly *et al.*, "An image is worth 16x16 words: Transformers for image recognition at scale," *arXiv preprint arXiv:2010.11929*, 2020.
- [38] Z. Liu, Y. Lin, Y. Cao, H. Hu, Y. Wei, Z. Zhang, S. Lin, and B. Guo, "Swin transformer: Hierarchical vision transformer using shifted windows," in *Int. Conf. Comput. Vis.*, 2021, pp. 10 012–10 022.
- [39] Z. Wang, X. Cun, J. Bao, W. Zhou, J. Liu, and H. Li, "Uformer: A general u-shaped transformer for image restoration," in *IEEE Conf. Comput. Vis. Pattern Recog.*, 2022, pp. 17 683–17 693.
- [40] X. Zhang, H. Zeng, S. Guo, and L. Zhang, "Efficient long-range attention network for image super-resolution," in *Eur. Conf. Comput. Vis.*, 2022.
- [41] J. Cao, J. Liang, K. Zhang, Y. Li, Y. Zhang, W. Wang, and L. V. Gool, "Reference-based image super-resolution with deformable attention transformer," in *Eur. Conf. Comput. Vis.*, 2022.
- [42] Z. Chen, Y. Zhang, J. Gu, Y. Zhang, L. Kong, and X. Yuan, "Cross aggregation transformer for image restoration," in *Adv. Neural Inform. Process. Syst.*, 2022.
- [43] J. Xiao, X. Fu, F. Wu, and Z.-J. Zha, "Stochastic window transformer for image restoration," in *Adv. Neural Inform. Process. Syst.*, 2022.
- [44] J. Xiao, X. Fu, A. Liu, F. Wu, and Z.-J. Zha, "Image de-raining transformer," *IEEE Trans. Pattern Anal. Mach. Intell.*, 2022.
- [45] Y. Song, Z. He, H. Qian, and X. Du, "Vision transformers for single image dehazing," *IEEE Trans. Image Process.*, vol. 32, pp. 1927–1941, 2023.
- [46] S. Chen, T. Ye, Y. Liu, E. Chen, J. Shi, and J. Zhou, "Snowformer: Scale-aware transformer via context interaction for single image desnowing," *arXiv preprint arXiv:2208.09703*, 2022.
- [47] D. Lepikhin, H. Lee, Y. Xu, D. Chen, O. Firat, Y. Huang, M. Krikun, N. Shazeer, and Z. Chen, "Gshard: Scaling giant models with conditional computation and automatic sharding," *arXiv preprint arXiv:2006.16668*, 2020.
- [48] W. Fedus, J. Dean, and B. Zoph, "A review of sparse expert models in deep learning," *arXiv preprint arXiv:2209.01667*, 2022.
- [49] D. Lepikhin, H. Lee, Y. Xu, D. Chen, O. Firat, Y. Huang, M. Krikun, N. Shazeer, and Z. Chen, "Gshard: Scaling giant models with conditional computation and automatic sharding," *arXiv preprint arXiv:2006.16668*, 2020.

- [50] J. Ma, Z. Zhao, X. Yi, J. Chen, L. Hong, and E. H. Chi, "Modeling task relationships in multi-task learning with multi-gate mixture-of-experts," in *ACM SIGKDD Int. Conf. Knowl. Discov. Data Mining*, 2018, pp. 1930–1939.
- [51] S. Kudugunta, Y. Huang, A. Bapna, M. Krikun, D. Lepikhin, M.-T. Luong, and O. Firat, "Beyond distillation: Task-level mixture-of-experts for efficient inference," *arXiv preprint arXiv:2110.03742*, 2021.
- [52] S. Gururangan, M. Lewis, A. Holtzman, N. A. Smith, and L. Zettlemoyer, "Demix layers: Disentangling domains for modular language modeling," *arXiv preprint arXiv:2108.05036*, 2021.
- [53] C. Riquelme, J. Puigcerver, B. Mustafa, M. Neumann, R. Jenatton, A. Susano Pinto, D. Keysers, and N. Houlsby, "Scaling vision with sparse mixture of experts," *Adv. Neural Inform. Process. Syst.*, vol. 34, pp. 8583–8595, 2021.
- [54] Z. Liu, H. Hu, Y. Lin, Z. Yao, Z. Xie, Y. Wei, J. Ning, Y. Cao, Z. Zhang, L. Dong *et al.*, "Swin transformer v2: Scaling up capacity and resolution," in *IEEE Conf. Comput. Vis. Pattern Recog.*, 2022, pp. 12 009–12 019.
- [55] L. Wu, M. Liu, Y. Chen, D. Chen, X. Dai, and L. Yuan, "Residual mixture of experts," *arXiv preprint arXiv:2204.09636*, 2022.
- [56] M. Emad, M. Peemen, and H. Corporaal, "Moesr: blind super-resolution using kernel-aware mixture of experts," in *IEEE Winter Conf. Appl. Comput. Vis.*, 2022, pp. 3408–3417.
- [57] J. Liang, H. Zeng, and L. Zhang, "Efficient and degradation-adaptive network for real-world image super-resolution," in *Eur. Conf. Comput. Vis.*, 2022, pp. 574–591.
- [58] W. Fedus, B. Zoph, and N. Shazeer, "Switch transformers: Scaling to trillion parameter models with simple and efficient sparsity," 2021.
- [59] L. Wang, Y. Wang, X. Dong, Q. Xu, J. Yang, W. An, and Y. Guo, "Unsupervised degradation representation learning for blind super-resolution," in *IEEE Conf. Comput. Vis. Pattern Recog.*, 2021, pp. 10 581–10 590.
- [60] K. He, H. Fan, Y. Wu, S. Xie, and R. Girshick, "Momentum contrast for unsupervised visual representation learning," in *IEEE Conf. Comput. Vis. Pattern Recog.*, 2020, pp. 9729–9738.
- [61] P. Khosla, P. Teterwak, C. Wang, A. Sarna, Y. Tian, P. Isola, A. Maschinot, C. Liu, and D. Krishnan, "Supervised contrastive learning," *Adv. Neural Inform. Process. Syst.*, vol. 33, pp. 18 661–18 673, 2020.
- [62] W. Wang, E. Xie, X. Li, D.-P. Fan, K. Song, D. Liang, T. Lu, P. Luo, and L. Shao, "Pyramid vision transformer: A versatile backbone for dense prediction without convolutions," in *Int. Conf. Comput. Vis.*, 2021, pp. 568–578.
- [63] S. Ren, D. Zhou, S. He, J. Feng, and X. Wang, "Shunted self-attention via multi-scale token aggregation," in *IEEE Conf. Comput. Vis. Pattern Recog.*, 2022, pp. 10 853–10 862.
- [64] C. Szegedy, W. Liu, Y. Jia, P. Sermanet, S. Reed, D. Anguelov, D. Erhan, V. Vanhoucke, and A. Rabinovich, "Going deeper with convolutions," in *IEEE Conf. Comput. Vis. Pattern Recog.*, 2015, pp. 1–9.
- [65] J. Johnson, A. Alahi, and L. Fei-Fei, "Perceptual losses for real-time style transfer and super-resolution," in *Eur. Conf. Comput. Vis.* Springer, 2016, pp. 694–711.
- [66] K. Simonyan and A. Zisserman, "Very deep convolutional networks for large-scale image recognition," *arXiv preprint arXiv:1409.1556*, 2014.
- [67] R. Li, L.-F. Cheong, and R. T. Tan, "Heavy rain image restoration: Integrating physics model and conditional adversarial learning," in *IEEE Conf. Comput. Vis. Pattern Recog.*, 2019, pp. 1633–1642.
- [68] R. Qian, R. T. Tan, W. Yang, J. Su, and J. Liu, "Attentive generative adversarial network for raindrop removal from a single image," in *IEEE Conf. Comput. Vis. Pattern Recog.*, 2018, pp. 2482–2491.
- [69] Y.-F. Liu, D.-W. Jaw, S.-C. Huang, and J.-N. Hwang, "Desnownet: Context-aware deep network for snow removal," *IEEE Trans. Image Process.*, vol. 27, no. 6, pp. 3064–3073, 2018.
- [70] M. Cordts, M. Omran, S. Ramos, T. Rehfeld, M. Enzweiler, R. Benenson, U. Franke, S. Roth, and B. Schiele, "The cityscapes dataset for semantic urban scene understanding," in *IEEE Conf. Comput. Vis. Pattern Recog.*, 2016, pp. 3213–3223.
- [71] N. Shazeer, A. Mirhoseini, K. Maziarz, A. Davis, Q. Le, G. Hinton, and J. Dean, "Outrageously large neural networks: The sparsely-gated mixture-of-experts layer," *arXiv preprint arXiv:1701.06538*, 2017.